Charge-density-wave gaps of $NbSe_3$ measured by point-contact spectroscopy in different crystallographic orientations

A. A. Sinchenko
Moscow State Engineering-Physics Institute, 115409 Moscow, Russia

P. Monceau
Centre de Recherches sur les tres Basses Temperatures, Boîte Postale 166, 38042 Grenoble, France

(Received 27 September 2002; published 19 March 2003)

We have measured the differential current-voltage (IV) characteristics of normal-metal (Au, Cu, In)-$NbSe_3$ direct point contacts (without insulating barrier) formed along different crystallographic orientations. For all investigated directions, at low temperature we clearly observed two charge-density-wave gaps Δ_{p1} and Δ_{p2} as excess resistance singularities in the IV curves. The excess resistance is attributed to the reflection of injected carriers from the normal metal on the Peierls energy gap barriers. The analysis of these results demonstrates the two-dimensional character of the electronic spectrum in $NbSe_3$ with a possible strong anisotropy of the energy gap in b-c plane.

DOI: 10.1103/PhysRevB.67.125117 PACS number(s): 71.45.Lr, 73.40.Ns, 74.45.+c

I. INTRODUCTION

One of the most important physical parameter of quasi-one-dimensional conductors with a charge-density-wave (CDW) ground state[1] is the energy gap opened in the single-particle excitation spectrum below the Peierls transition temperature T_p. Most of publications concerning energy-gap measurements in CDW's using tunneling spectroscopy (which is the direct method of studying density of states) are related mainly to $NbSe_3$.[2–6] The interest for this material is defined by its special properties. Indeed, in most materials with a CDW, the formation of the Peierls energy gap yields a complete destruction of the Fermi surface, resulting in a semiconducting ground state at temperatures below T_p.[1] However, $NbSe_3$ exhibits a metallic behavior down to very low temperatures. This behavior has been understood by the existence of normal carriers in small pockets remaining below the two CDW phase transitions at $T_{p1}=144$ K and $T_{p2}=59$ K (Refs. 7 and 8) because of the lack of perfect nesting between portions of the Fermi surface connected by the distortion-wave vector. The unit cell of $NbSe_3$ in the a^*-c plane is made up of three pairs of chains. Band calculations[9] of $NbSe_3$ demonstrate that the T_{p1}-CDW transition is attributable to a nearly perfect nesting and is associated with a pair of chains. It was conjectured that the CDW with its onset at $T_{p2}=59$ K occurs on the second and third pair of chains, but with an imperfect nesting. At $T<T_{p2}$ two energy gaps, corresponding to the first ($2\Delta_{p1}$) and the second ($2\Delta_{p2}$) Peierls transition are opened; but at the same time, normal-metal properties remain. These features allow the expectation of a very interesting behavior of the density of states in $NbSe_3$.

In spite of a great attention to this material, the results obtained up to now do not allow to make definite conclusions about the energy-gap behavior. Indeed, in most cases the experiments were carried out only at $T=4.2$ K and only in the direction along the a^* axis, i.e., perpendicular to the chain direction,[2–5] and thus there are no direct informations about gap anisotropy. But, because of the nonperfect nesting and the presence of normal carriers in $NbSe_3$, it may be expected that along some directions in k space the energy gap is zero. The determination of these directions appears to be of a great interest.

Values of energy gaps obtained from previous experiments vary significantly: $\Delta_{p2}\approx 23-37$ meV and $\Delta_{p1}\approx 50-100$ meV.[3–6] It should be noted that in Ref. 3 it was concluded that the real CDW density of states is composed of a distribution of gaps, possibly because of the strong anisotropy. For all cases the observed $2\Delta_p/k_BT_p\simeq 8.2-14.4$ instead of 3.52 as expected from a mean-field BCS-type theory. This discrepancy is usually attributed to inherent strong fluctuations in quasi-one-dimensional systems.[10] Another explanation has been proposed by Huang and Maki.[11] Assuming that the electron spectrum in $NbSe_3$ is two dimensional, their calculation of density of states are in a good agreement with the experimental results reported in Ref. 2. The assumption about the two-dimensional character of the electronic spectrum in $NbSe_3$ was confirmed in Ref. 12, where the electrical transport along the a^* axis was investigated. From the results obtained, it was assumed that the CDW condensation is localized in the b-c plane in elementary conducting layers spatially separated by atomically thin insulating layers. The CDW order parameter is modulated along the a^* axis, and the transport across the layers is determined by the intrinsic interlayer tunneling. In the frame of this model of $NbSe_3$ stacked junctions the Peierls energy gap is opened only in b-c plane. To prove this hypothesis energy-gap measurements in different directions need to be performed.

The very small sizes in the transverse directions of $NbSe_3$ single crystals make that high quality tunnel junctions are very difficult to be prepared. In most cases the planar CDW-I-S (I-insulator, S-superconductor) or CDW-I-N (N-normal metal) junctions were investigated. Using a superconducting counterelectrode gives the possibility to verify the quality of the insulating barriers in observing the superconducting energy-gap singularity.[5] But the surface quality of the CDW material, which is more important, remains undefined. The indication of a nongood surface state may be derived by the

 ©2003 The American Physical Society

fact that all obtained CDW gap structures are substantially broadened when compared with those from the BCS prediction. This brief analysis shows that the determination of the energy gaps in $NbSe_3$ remains largely unsolved, that has been the motivation of this present work.

We have used an original method of energy-gap spectroscopy, based on the investigation of *IV* characteristics of direct-type junctions (without any insulating layer). This technique has been already used in Ref. 6 for the determination of the energy gap in $NbSe_3$ single crystals, but in the temperature range 77–300 K only. The method is based on reflection of injected carriers from the normal metal on barriers associated with the Peierls energy gap in direct normal-metal-CDW contacts (*N*-CDW) when their energy is less than Δ_p, as it was shown theoretically[13,14] and experimentally.[15,16] In Ref. 13 the mechanism of transformation of injected carriers into the CDW condensate was proposed. It was shown that the electron-hole pairs moving from the *N*-CDW interface carry away twice the momentum of an electron incident normal to the interface. In Ref. 14 it was concluded that the result of injection of carriers from the normal metal is mainly a mirror reflection. But for both cases the result of interaction between injected particles and the CDW is a reflection the manifestation of which is the appearance of an excess resistance at the *N*-CDW interface for $V \leqslant \Delta_p/e$, thus giving the possibility to directly determine the energy gap from the *N*-CDW point-contact characteristics.

The injection of carriers through Sharvin-type point contacts[17] takes place in all directions. But, as it was shown in Ref. 18, these point contacts are directional with respect to the electric-field configuration, and, in the isotropic case, the main contribution to the point-contact resistance comes from injection along the point-contact orientation. So, measurements of characteristics of point contacts in different orientations give some information about the anisotropic properties of the density of states. Hereafter, we report detailed energy-gap measurements in $NbSe_3$ along a^*-, *b*-, and *c*-axis directions in the temperature range 2.5–65 K.

II. EXPERIMENTAL TECHNIQUE

The $NbSe_3$ samples selected for experiments had a size along *b* axis $L_b \approx 3$–4 mm, along *c* axis L_c approx. 10–50 μm and along a^*- axis $L_a \approx 1$ μm. The temperatures of the upper Peierls transition $T_{p1} = 144$ K and the lower one $T_{p2} = 59$ K were determined from the temperature dependence of the resistance.

The very small thickness of the $NbSe_3$ samples makes practically impossible the formation of a point contact along *b*-axis and *c*-axis direction using the conventional metallic needle-type tip. Therefore, as a tip, we used a thin gold strip of 50 μm width, and thickness of 4 μm. For a^*-axis direction, we used electrochemically etched thin metal (Au, Cu, In) wires as a counterelectrode. The tip diameter was less than 1 μm. The appropriate contact geometry is shown in Fig. 1.

The electrical contact of the sample with the normal-metal counterelectrode was formed at low temperature with the use of a mechanical motion transfer system of a great precision.

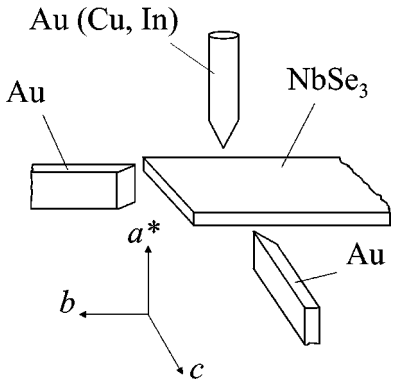

FIG. 1. The scheme of the experimental set up.

The measurements of the *IV* characteristics and its first derivative $R_d = dV/dI$, were carried out with the standard modulation technique.

Reliable energy-gap spectroscopy by means of point contacts is possible if the mean free path *l* of conduction electrons is larger than the size of the contact (ballistic regime). In this case, electrons cross the contact ballistically, gaining the whole energy *eV*, and can loose this energy in collisions with excitations. The resistance in the ballistic regime is given by the well-known Sharvin formula:[17]

$$R_{con} = \frac{\rho l}{d^2}, \tag{1}$$

where ρ is the resistivity and *d* is the contact diameter. The point contacts we investigated had resistances at zero bias between 20 and 1000 Ω. Taking $\rho = 10^{-5}$ Ωcm and $l = 10^{-4}$ cm (Ref. 19), we estimate the diameter of point contact with the lowest resistance to be $d \lesssim 10^{-5}$ cm, that is less than the mean free path. Therefore, we never have a situation with $l < d$, when a contact is in the thermal regime.

The expected nonlinearities in *IV* curves generally may have three causes: (i) energy-gaps singularities; (ii) the possible local CDW deformation (sliding) in the contact region because of a large electric field; and (iii) the Joule heating. The last may be easily determined from the shape of *IV* curves at high voltages. The deformation of the CDW plays an important role for materials with a semiconducting ground state. For these materials the electric field in the vicinity of a *N*-CDW point contact penetrates into the CDW on a macroscopic length, leading to a band bending effect of a large amplitude. The consequence of it is a significant nonsymmetry of the *IV* curves of the *N*-CDW point contacts.[20] But, in the case of $NbSe_3$, the screening by the remaining normal carriers is effective. So, we can expect that this effect will be negligible in our experiments.

III. EXPERIMENTAL RESULTS

Examples of the most typical differential *IV* characteristics for point-contacts oriented along a^*, *b*, and *c* axis at $T \lesssim 4.2$ K are shown in Fig. 2. It may be seen that, for all curves, the increment of R_d at high voltages ($V > 100$ mV) is proportional to the square of the bias voltage, that is typical

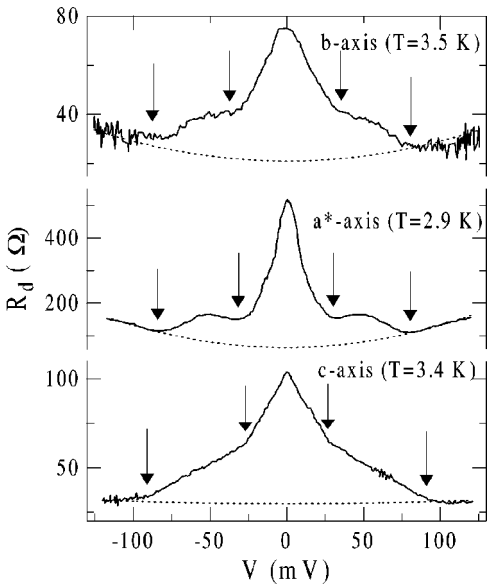

FIG. 2. Typical dependencies of the differential resistance $R_d(V)$ for contacts oriented along *b*-, *a**-, and *c*-axis directions measured at $T<4.2$ K. The voltages corresponding to the energy-gap positions are indicated by arrows. The dotted line is the normal-state background curve.

for Joule heating of a metal-metal contact (dotted lines in Fig. 2). It is quite different from tunnel-type *IV* curves for which the increment of resistance $\delta R_d(V)\sim 1/V^2$ (Ref. 21). This fact demonstrates, indeed, that these investigated contacts are of a direct type (without insulating barrier).

For all curves shown, at $|V|<100$ mV, the differential resistance increases in two steps, to its maximum when $V=0$. We associate these two step maxima with the excess resistance arisen from the reflection of injected quasiparticles on the Peierls energy-gap barriers. The first step in the excess resistance, corresponding to the carrier reflection on the first Peierls gap Δ_{p1} takes place at $|V_1|\approx 75$–80 mV for *b*, 85–95 mV for *c*, and 65–80 mV for *a**-axis oriented contacts. The second step is connected with the second Peierls gap Δ_{p2} and occurs at $|V_2|\approx 28$–34 mV for *b*- and *c*-axis oriented contacts, and 24–30 mV for *a**-axis oriented contacts. Indeed, the measured magnitudes of eV_1 and eV_2 corresponding to these singularities are in agreement with the value of the first and the second energy gap of $NbSe_3$ determined earlier.[3–6] It can be seen from Fig. 2 that the shape of the excess resistance maximum is nearly the same for contacts oriented along *b* and *a** axis. The resistance starts to increase when the voltage is decreased below $V=\Delta_{p1}/e$ and has a tendency of saturation at low voltages. The same picture is observed at $V<\Delta_{p2}/e$. A qualitatively different picture is observed for *c*-axis oriented contacts. R_d starts practically linearly to increase with decreasing voltage from $V\simeq\Delta_{p1}/e$ and, of variance with the other investigated directions, there are no tendency of saturation at low voltages. A linear increase of R_d with another slope, without tendency of saturation, is also observed in the voltage range from $V\approx\Delta_{p2}/e$ down to $V=0$.

To make clear the effect of carrier reflection on the

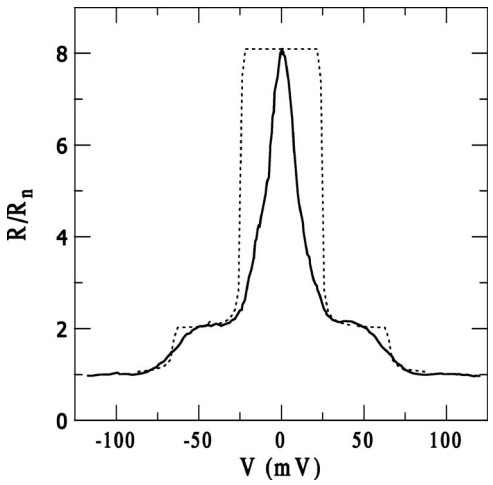

FIG. 3. Normalized differential resistance $R_d(V)/R_{dN}(V)$ measured at $T=3.8$ K for a contact Au-$NbSe_3$ oriented along *a** axis. The dotted line is the theoretical fit with $\Delta_{p1}=65.0$ mV and $\Delta_{p2}=24.5$ mV.

energy-gap barriers, we have normalized the $R_d(V)$ curves to the normal-state background curves (shown as dotted lines in Fig. 2). The result of this procedure for a contact oriented along *a** axis at $T=3.8$ K is shown in Fig. 3 (solid line). The relative amplitude of the excess resistance at zero bias $R_d(0)/R_{dN}(0)$, where R_{dN} is the background resistance, is 3.5–9.5 for *a**- and *b*-axis, and 1.4–2.7 for *c*-axis oriented contacts.

The temperature evolution of the normalized $R_d(V)$ dependence is shown in Fig. 4 for one of the *a**-axis contact. It can be seen that, when the temperature is increased, the amplitude of the second step in the excess resistance decreases and its voltage position goes monotonically to zero; this step vanishes completely at $T=59$ K, corresponding to the second Peierls transition temperature. At the same time the volt-

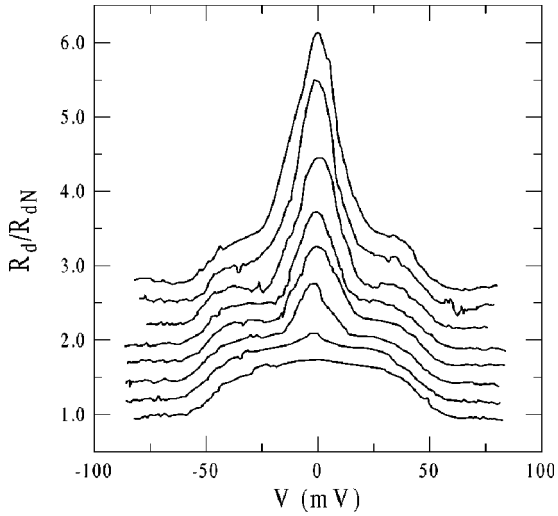

FIG. 4. $R_d/R_{dN}(V)$ curves for a contact In-$NbSe_3$ oriented along *a**-axis direction at $T=4.2$, 29.5, 48.2, 50.5, 52.6, 54.6, 58.3, and 60.4 K. The resistance scale corresponds to the curve at 60.4 K, the other curves are offset for clarity.

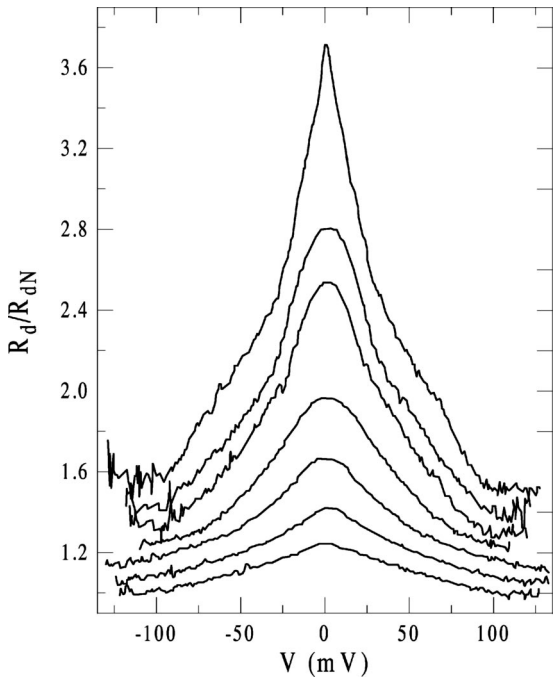

FIG. 5. $R_d/R_{dN}(V)$ curves for a contact Au-$NbSe_3$ oriented along *c*-axis direction at $T=3.5$, 19.8, 44.0, 50.1, 52.7, 56.1, and 59.5 K. The resistance scale corresponds to the curve at 59.5 K, the other curves are offset for clarity.

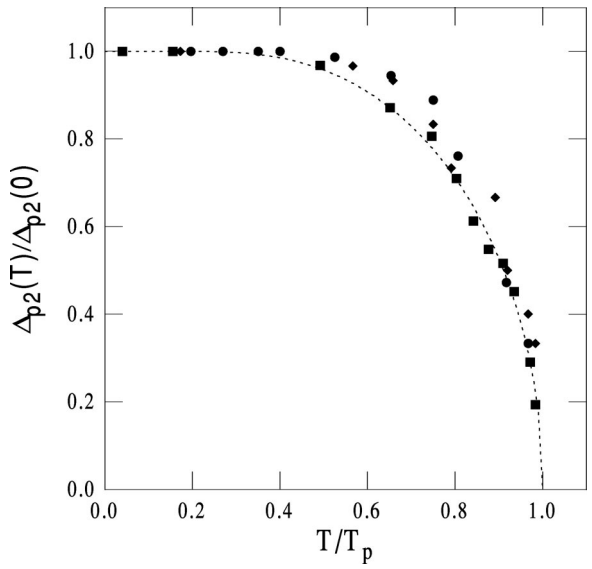

FIG. 6. The temperature dependence of the low-temperature CDW energy gap in $NbSe_3$ obtained for different contacts oriented along a^* axis. The different symbols correspond to different point contacts. The dashed curve corresponds to the BCS theory.

age position and the amplitude of the first step in the excess resistance remains practically unchanged in this temperature range (in accordance with the BSC-theory prediction). Indeed, according to this model, the first Peierls gap is practically independent of temperature in this temperature range. The same behavior is observed for *b*-axis contacts. But, because of the lack of stability of contacts in this direction, we did not succeed in obtaining the temperature evolution of $R_d(V)$ curves in the full temperature range for the same point contact.

The temperature evolution of the normalized $R_d(V)$ dependence for a *c*-axis oriented contact is shown in Fig. 5. In contrast to the a^*- and *b*-axis oriented contacts, the second step in the excess resistance is smeared out with the temperature increasing and the voltage position of this resistance maximum becomes undeterminable. The voltage position of the first step remains unchanged, but the amplitude of this resistance maximum significantly decreases when the temperature is increased.

Figure 6 shows the normalized temperature dependence of the second Peierls energy gap for several different contacts oriented along *b*- and a^*-axis directions, determined as the voltage at which $R_d(V)$ is minimum (shown by arrows in Fig. 2). It can be seen, that the experimental results are in a good agreement with the temperature dependence of the energy gap following the BCS theory, indicated in the figure by a dotted line.

IV. DISCUSSION

Let us first analyze the shape of point-contact spectra obtained for *b*- and a^*-axis oriented contacts. As it was mentioned above, the shape of point-contacts spectra along these directions is qualitatively the same. It can be seen from Fig. 3 that, for such directions, the result of the interaction of injected quasiparticles from the normal metal with the Peierls energy-gap appears in the *IV* curves as an excess resistance at $|eV|<\Delta$. That is quite different from the tunnel-type junction where the energy gap singularity appears as a sharp minimum at $|eV|=\Delta$, demonstrating the features of the BCS tunnel density of states which diverges at $\pm\Delta$. The behavior we observed in our experiments is in a qualitative agreement with models predicting the reflection of normal carriers from the energy-gap barrier at the normal-metal-CDW interface.[13,14]

For all investigated contacts, we observed simultaneously the energy-gap singularities corresponding to the low- and high-temperature CDW of $NbSe_3$. It is the indication that the first and the second Peierls transitions take place on different types of chains. Therefore, we can model our contact as two CDW's connected in parallel and a normal metal corresponding to uncondensed carriers. Then the total current through the contact, I_t, is the sum of three currents

$$I_t=I_{p1}+I_{p2}+I_n, \tag{2}$$

where I_{p1}, I_{p2} are the currents flowing through the parts of the contact including the first and the second CDW, and I_n is the current of the remaining normal carriers (not normal excitations of the CDW's). We assume that $I_n(V)$ follows the Ohmic law and that the $I_p(V)$ dependencies may be calculated as

$$I_p(V)=N(0)ev_F A\int_{-\infty}^{\infty}[f_0(E-eV)-f_0(E)]D(E)dE, \quad (3)$$

where $f_0(E)$ is the electron distribution function, $N(0)$ is the density of states at the Fermi level ε_F, A is the effective cross-section area corresponding to transport through the given CDW and $D(E)$ is the transmission coefficient, which depends on the corresponding CDW energy gap. The parameter A is proportional to the relative number of chains of a given type included in the contact. This parameter determines the relation between the amplitudes of the first and the second excess resistance maxima which are different for different point contacts.

Modeling the energy gap as a potential step with a height equal to Δ_p, we can consider our point-contact as a quantum-mechanical task about the scattering of a particle on such a type barrier. The transmission coefficient obtained from the solution of the Schrödinger equation is $D(E)=0$ at $E\leqslant\Delta_p$ and

$$D(E)=\frac{4\sqrt{E(E-\Delta_p)}}{(\sqrt{E}+\sqrt{E-\Delta_p})^2}, \quad \text{for} \quad E>\Delta_p. \quad (4)$$

We do not consider in this simple model the influence of a possible nonideality of the N-CDW boundary. As a first approximation, we have also assumed that the normal-state differential conductivity for all types of chains is the same and the dI_n/dV is energy independent. In this case, only the parameters A and Δ_p are variable. Following this model, the curve shown in Fig. 3 by a dotted line is obtained with $\Delta_{p1}=65.0$ meV and $\Delta_{p2}=24.5$ meV. It can be seen from the figure that a discrepancy with the theory is observed for both energy gaps. For example, the experiment shows that the conductivity of contacts starts to increase from very low voltages, even at very low temperatures.

The observed shapes of excess resistance maxima are in a qualitative agreement with the Huang and Maki calculations[11] of the density of states in $NbSe_3$ assuming a two-dimensional electronic spectrum. The same conclusion about the two-dimensional character of the electron spectrum in $NbSe_3$ was made in Ref. 12. In this case, the energy gap is absent in the direction transverse to b-c plane. But, in the present work, we have clearly observed energy-gap singularities in point-contacts spectra along a^*-axis direction. This disagreement can be eliminated if we take into account the large conductivity anisotropy of $NbSe_3$. According to Ref. 22, at low temperatures, the conduction ratio $\sigma_b/\sigma_{a*}\sim 10^4$. Therefore, the electric-field distribution is strongly modified in the contact region with respect to the isotropic case. For contacts oriented along a^* axis, because of the very large anisotropy, the preferable direction for the carrier injection is along b axis. It is the explanation why the obtained spectra for contacts oriented along b and a^* are qualitatively the same. Actually, it follows from our experiments that the contacts along a^* axis, in fact, probe the density of states along b-axis direction. Therefore, we can conclude that the results obtained do not contradict the assumption about the two-dimensional character of the electronic spectrum in $NbSe_3$.

Let us consider now the energy-gap behavior in b-c plane. From the comparison of the IV curves of point contacts oriented along b and c axis we can note three features. First, as it was mentioned above, the shape of excess resistance maxima for c-axis contacts differ qualitatively from those along b-axis direction. Second, the temperature evolution of $R_d(V)$ characteristics of c-axis contacts is also different from a^*- and b-axis oriented contacts (see Figs. 4 and 5). Third, the mean value of the relative amplitude of excess resistance maximum for c-axis oriented contacts is more than three times less than for b-axis direction. At the same time the conductivity ratio $\sigma_b/\sigma_c\simeq 10$ (Ref. 19) is not very large and the direction along c axis remains as the preferable injection direction.

The nature of such a behavior is unclear, but one possible explanation may be obtained with the assumption that Δ_p is strongly anisotropic in b-c plane, and the energy gap is close to zero near the c-axis direction. Indeed, the observed excess resistance for c-axis direction should depend, in this case, on contributions from carrier injection along directions which are different from c-axis direction. If Δ_p increases for directions away from c-axis direction, then we will observe a smeared maximum of the excess resistance, the shape of which depend on the angle energy-gap distribution. In this case, the amplitude of excess resistance maxima for c-axis oriented contacts should be less than for the other directions. This is that we really observed in our experiment. In the frame of this assumption, it becomes possible to also explain the temperature dependence of the amplitude of the first excess resistance maximum. As stipulated above, the main contribution to the point-contact differential resistance comes from the injection in directions which are close to c axis, corresponding to small energy-gap values. With temperature increasing the magnitudes of these small gaps become comparable with temperature, and the carriers can then start to penetrate into the CDW. The another reason for the assumption about a zero energy gap along some direction in the b-c plane may be the existence of noncondensed to CDW normal carriers. In this case the node direction corresponds to the direction of the normal carrier pockets. But for proving this hypothesis about a zero energy gap in the vicinity of c direction, further experiments need to be done; for example, low-temperature angle resolution photoemission spectroscopy of $NbSe_3$ single crystals is desirable.

V. CONCLUSION

In conclusion, we have investigated point-contact characteristics of a normal metal (Au, Cu, In) with a quasi-one-dimensional CDW conductor with, $NbSe_3$, in the temperature range from 2.5 K up to 65.0 K for different crystallographic orientations. It was shown that, for contacts without insulating barrier, the direct energy-gap spectroscopy

is possible. The specific feature of the differential *IV* characteristics of such type of contacts is an excess resistance corresponding to the reflection of injected carriers from the normal metal on the first and the second Peierls energy gaps of $NbSe_3$. The obtained temperature dependence of the second Peierls energy gap follows well the BCS theory. The results obtained point out to the two-dimensional character of the electronic spectrum of $NbSe_3$ with a strong energy-gap anisotropy in *b*-*c* plane.

ACKNOWLEDGMENTS

The authors are thankful to S. N. Artemenko, L. N. Bulaevski, Yu. I. Latyshev, and K. Maki for helpful discussions of these experimental results. The work was supported by Russian State Fund for the Basic Research (Grants No. 01-02-16321 and No. 02-02-17263) and INTAS (Grant No. 01-0474), and the twinning program No. 19 between CRTBT-CNRS and RAS.

[1] G. Grüner, *Density Waves in Solids* (Addison-Wesley, Reading, Massachusetts, 1994); L. Gor'kov and G. Grüner *Charge Density Waves in Solids* (Elsevier Science, Amsterdam, 1989); *Electronic Crystals 99*, edited by S. Brazovskii and P. Monceau (Editions de Physique, France, 1999).

[2] T. Ekino and J. Akimitsu, J. Appl. Phys. **26**, 625 (1987).

[3] T. Ekino and J. Akimitsu, Physica B **194-196**, 1221 (1994).

[4] Zhenxi Dai, C.G. Slough, and R.V. Coleman, Phys. Rev. Lett. **66**, 1318 (1991); Zhenxi Dai, C.G. Slough, and R.V. Coleman, Phys. Rev. B **45**, 9469 (1992).

[5] A. Fournel, J.P. Sorbier, M. Konczykovski, and P. Monceau, Phys. Rev. Lett. **57**, 2199 (1986); J.P. Sorbier, H. Tortel, P. Monceau, and F. Levy, *ibid.* **76**, 676 (1996).

[6] A.A. Sinchenko, Yu.I. Latyshev, S.G. Zybtsev, I.G. Gorlova, and P. Monceau, Phys. Rev. B **60**, 4624 (1999).

[7] P. Monceau, N.P. Ong, A.M. Portis, A. Meershant, and J. Rouxel, Phys. Rev. Lett. **37**, 602 (1976).

[8] J.A. Wilson, Phys. Rev. B **19**, 6456 (1979).

[9] N. Shima and H. Kamimura, in *Theoretical Aspects of Band Structures and Electronic Properties of Pseudo-One-Dimensional Solids*, edited by H. Kamimura (Reidel, Boston, 1985).

[10] Y. Suzumura, Jpn. J. Appl. Phys., Part 1 **26**, 607 (1987).

[11] X.-Z. Huang and K. Maki, Phys. Rev. B **40**, 2575 (1989).

[12] Yu.I. Latyshev, A.A. Sinchenko, L.N. Bulaevski, V.N. Pavlenko, and P. Monceau, Pis'ma Zh. Éksp. Teor. Fiz. **75**, 93 (2002) [JETP Lett. **75**, 103 (2002)].

[13] M.I. Visscher and G.E.W. Bauer, Phys. Rev. B **54**, 2798 (1996); B. Rejaei and G.E.W. Bauer, *ibid.* **54**, 8487 (1996).

[14] S.N. Artemenko and S.V. Remizov, Pis'ma Zh. Éksp. Teor. Fiz. **65** 50 (1997) [JETP Lett. **65**, 53 (1997)].

[15] A.A. Sinchenko, Yu.I. Latyshev, S.G. Zybtsev, I.G. Gorlova, and P. Monceau, Pis'ma Zh. Éksp. Teor. Fiz. **64**, 259 (1996) [JETP Lett. **64**, 285 (1996)].

[16] A.A. Sinchenko, Yu.I. Latyshev, S.G. Zybtsev, and I.G. Gorlova, Zh. Éksp. Teor. Fiz. **113**, 1830 (1998) [JETP **86**, 1001 (1998)].

[17] Yu.V. Sharvin, Zh. Éksp. Teor. Fiz. **48**, 984 (1965) [Sov. Phys. JETP **21**, 655 (1965)].

[18] I.O. Kulik, A.N. Omel'yanchuk, and R.I. Shekhter, Fiz. Nizk. Temp. **3**, 1543 (1977) [Sov. J. Low Temp. Phys. **3**, 740 (1977)].

[19] N.P. Ong, Phys. Rev. B **18**, 5272 (1978); N.P. Ong and J.W. Brill, *ibid.* **18**, 5265 (1978).

[20] A.A. Sinchenko, V.Ya. Pokrovskii, and S.G. Zybtsev, Pis'ma Zh. Éksp. Teor. Fiz. **74**, 191 (2001), [JETP Lett. **74**, 173 (2001)].

[21] E.L. Wolf, *Principles of Electron Tunneling Spectroscopy* (Oxford University Press, New York/Clarendon Press, Oxford, 1985).

[22] Yu.I. Latyshev, P. Monceau, O. Laborde, B. Pennetier, V.N. Pavlenko, and T. Yamashita, J. Phys. IV **9**, 165 (1999).